New insights into the exploitation of oxidized carbon nitrides as heterogeneous base catalysts

Giuseppe Gentile [a], Cristian Rosso [a], Alejandro Criado [b], Valentina Gombac [c], Giacomo Filippini [a,*], Michele Melchionna [a,c,*], Paolo Fornasiero [a,c,*], Maurizio Prato [a,c,d,e,*]

[a] Department of Chemical and Pharmaceutical Sciences, University of Trieste, Via L. Giorgieri 1, Trieste 34127, Italy
[b] Universidade da Coruña, Centro de Investigacións Científicas Avanzadas (CICA), Rúa as Carballeiras, 15071, A Coruña, Spain
[c] Consorzio Interuniversitario Nazionale per la Scienza e Tecnologia dei Materiali (INSTM), Unit of Trieste, via L. Giorgieri 1, Trieste 34127, Italy
[d] Center for Cooperative Research in Biomaterials (CIC biomaGUNE), Basque Research and Technology Alliance (BRTA), San Sebastián, Spain
[e] Ikerbasque, Basque Foundation for Science, Bilbao, Spain

ARTICLE INFO

Keywords:
Synthetic methods
Heterogeneous catalysis
Materials science
Organocatalysis
Surface analysis

ABSTRACT

In this work, the development of a novel efficient heterogeneous catalytic system capable of driving Knoevenagel condensation reactions between benzaldehydes and malononitrile was reported. Specifically, we explored a post-synthetic modification of graphitic carbon nitride (g-CN) through a strong oxidation treatment by acid mixture (HNO_3/H_2SO_4). The as-prepared oxidized CN material (CNO) shows a large number of surface acidic moieties, that can be easily deprotonated through an aqueous alkaline wash with different bases (NaOH, K_2CO_3, *t*-BuOK), to introduce a high density of reactive basic sites. The best catalyst is obtained with NaOH as the base (CNO-*NaOH*), and displays high reactivity and good tolerance towards functional group variations of the reagents, thus emerging as a potential new recyclable carbon nitride-based structure for organic base catalysis.

1. Introduction

Base catalysis for organic reactions represents one of the classical topics found in all undergraduates' organic chemistry textbooks. The use of bases can trigger several carbon-carbon coupling processes of great importance in organic syntheses, such as the Knoevenagel condensations, transesterifications, aldol condensations and others.[1–3] The Knoevenagel condensation is an essential process giving access to α-β unsaturated products, which are critical for a variety of industrial sectors.[4,5] To circumvent the typical drawbacks of homogeneous catalysis, efforts have been devoted to the development of heterogeneous Knoevenagel reaction catalysts, where the base catalytic sites are anchored to solid supports. This strategy, which is of general applicability in organic synthesis, bears several advantages such as the ease of catalyst recyclability and product separation, the possibility to work under higher temperatures, and the avoidance of excess solvent and waste.[6–9] In the wake of the modern policy on implementing sustainability in chemical production, an obvious objective has been to prepare metal-free heterogeneous catalysts, because of their favorable production economy and higher environmental compatibility.[10–12] As a matter of fact, transition metal-based catalytic systems are, generally, expensive and potentially toxic.[13] On the other hand, graphitic carbon nitride (g-CN) and its various structural variations have been proposed as a versatile metal-free heterogeneous catalyst to promote a variety of base-catalyzed reactions, due to the simplicity of its preparation and modification, as well as to the presence in its structure of nitrogen atoms with Lewis base character.[14–17] Use of g-CN in the Knoevenagel condensation has been proven to be a viable and simple avenue with a wide scope reaction, although intrinsic low surface areas of g-CN limit the productivity because of the low density of exposed catalytic sites.[18,19] Su et al. found that the activity of mesoporous carbon nitride (mpg-CN) towards Knoevenagel coupling could be significantly enhanced by treating the mpg-CN with strong bases. This was explained in terms of a further pre-activation following the deprotonation of the mpg-CN, which was protonated during the synthetic protocol.[20] Krishnan et al. investigated the use of oxidized carbon nitrides, produced from g-CN, to catalyse in heterogeneous phase the hydrogen transfer reaction of carbonyl compounds. Interestingly, they reported that oxidation treatments by strong oxidants $KMnO_4$, $K_2Cr_2O_7$ and H_2O_2 effectively instal oxygenated moieties on the surface of the

* Corresponding authors at: Department of Chemical and Pharmaceutical Sciences, University of Trieste, Via L. Giorgieri 1, Trieste 34127, Italy.
E-mail addresses: gfilippini@units.it (G. Filippini), melchionnam@units.it (M. Melchionna), pfornasiero@units.it (P. Fornasiero), prato@units.it (M. Prato).

Accepted 26 November 2021

material, and upon the addition of a base both the carbonyl compound and the hydrogen donor are coordinated to the oxidized carbon nitride allowing for the reaction to take place.[21] Thus, we envisaged that the introduction of acidic groups on the g-CN by means of facile oxidation protocols could allow the creation of additional basic sites after deprotonation with strong inorganic bases. Here, we employ a well-established oxidation protocol used in general for nanostructured carbon materials, namely oxidation with sulfonitric mixture to insert acidic oxygenated functional groups. The distribution of the different functional groups includes carboxylic acid and hydroxylic groups, which could be deprotonated with strong bases such as NaOH, *t*-BuOK, K_2CO_3. Importantly, the strong oxidative protocol also causes an enhancement of the surface area with respect to the original g-CN, increasing the efficiency of the catalytic process. As a result, the activity towards Knoevenagel coupling is enhanced to a great extent, surpassing by far that of conventional deprotonated g-CN. Moreover, we discovered that the type of base is critical for the resulting activity.

2. Experimental Section

2.1. General information

Carbon nitride (g-CN) was prepared in cubic muffle operating under static air atmosphere, with the sample positioned in the middle. Intrinsic pH of the materials and surface basic sites were determined using a Hach pH meter. UV-Vis measurements were carried out on Cary 5000 UV-Vis-NIR spectrophotometer. All the spectra were recorded at room temperature using 10 mm path-length cuvettes. Thermogravimetric analysis (TGA) was recorded with a TGA Q500 (TA instruments), under a flow of N_2 (90 mL min^{-1}), following a temperature program consisting in the equilibration of the sample at 100 °C followed by a ramp at 10 °C/min up to 800 °C. The sample aliquot ranged from 1 to 2 mg, exactly weighed. NMR spectra were recorded on Varian 400 and Varian 500 spectrometer (^{1}H: 400 MHz – 499 MHz and 376 MHz for ^{19}F). The chemical shifts (δ) for ^{1}H and ^{19}F are given in ppm relative to residual signals of the solvents ($CHCl_3$ @ 7.26 ppm ^{1}H NMR). Coupling constants are given in Hz. The following abbreviations are used to indicate the multiplicity: s, singlet; d, doublet; t, triplet; q, quartet; m, multiplet; br, broad signal. NMR yields were calculated by using trichloroethylene as internal standard. All organocatalytic reactions were set up in glass vials, unless otherwise stated. Chromatographic purification of products was accomplished using flash chromatography on silica gel (35–70 mesh). For thin-layer chromatography (TLC) analysis throughout this work, Merck pre-coated TLC plates (silica gel 60 GF254, 0.25 mm) were employed, using UV light as the visualizing agent (254 nm), basic aqueous potassium permanganate ($KMnO_4$) stain solution or iodine, and heat as developing agents. Organic solutions were concentrated under reduced pressure on a Büchi rotatory evaporator. XPS experiments were performed in a SPECS Sage HR 100 spectrometer with a non-monochromatic X ray source of Magnesium with a Kα line of 1253.6 eV energy and 250 W. The samples were placed perpendicular to the analyzer axis and calibrated using the 3d5/2 line of Ag with a full width at half maximum (FWHM) of 1.1 eV. An electron flood gun was used to compensate for charging during XPS data acquisition. The selected resolution was 30 and 15 eV of Pass Energy and 0.5 and 0.15 eV/step for the survey and high-resolution spectra, respectively. Measurements were made in an ultrahigh vacuum (UHV) chamber. Fitting of the XPS data were done using CasaXPS 2.3.16 PR 1.6 software. For our data, the Shirley-type background subtraction was used and all curves were defined as 40% Lorentzian, 60% Gaussian. Raman spectra were acquired using an Invia Renishaw spectrometer equipped with a diode laser at 785 nm.

Table 1
Optimized reaction conditions and control experiments. Reactions were performed on a 0.1 mmol scale. [a] Yield determined by ^{1}H NMR spectroscopy using 1,1,2-trichloroethene as the internal standard.

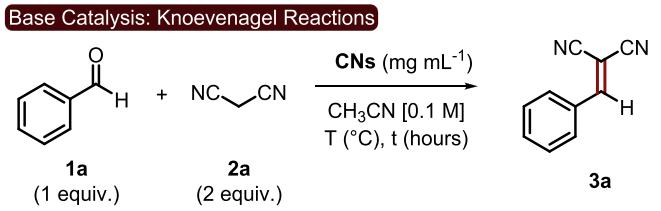

Entry	CNs (mg/mL)	t (h)	T (°C)	Yield 3a (%)[a]
1	-	16	70	0
2	g-CN (5)	16	70	0
3	CNO (5)	16	70	0
4	g-CN-*K_2CO_3* (5)	16	70	0
5	g-CN-*NaOH* (5)	16	70	0
6	g-CN-*tBuOK* (5)	16	70	0
7	CNO-*K_2CO_3* (5)	16	70	>99
8	CNO-*NaOH* (5)	16	70	>99
9	CNO-*tBuOK* (5)	16	70	>99
10	CNO-*K_2CO_3* (5)	16	25	62
11	CNO-*NaOH* (5)	16	25	83
12	CNO-*tBuOK* (5)	16	25	63
13	**CNO-*NaOH* (5)**	**2**	**70**	**>99**

2.2. Materials

Commercial reagents and solvents were purchased Sigma-Aldrich, Fluka, Alfa Aesar, Fluorochem, VWR and used as received, without further purification, unless otherwise stated. Melamine, benzaldehyde, 4-iodobenzaldehyde, 4-nitrobenzaldehyde, 4-cyanobenzaldehyde and 4-fluorobenzaldehyde were commercially available.

2.3. General procedures for the preparation of carbon nitrides

A general workflow for the preparation of CNs materials is available in the supporting information (SI) – Fig. S1.

2.3.1. Preparation of g-CN

g-CN. Melamine (10 g) was transferred in a covered alumina crucible and heated in muffle furnace at 550 °C for 300 min with a ramping time of 5 °C/min. The final product was milled to have a uniform powder.

2.3.2. Preparation of CNO

g-CN (500 mg) was treated with a mixture of concentrated nitric and sulfuric acid (2:1 v/v ratio, 100 mL) at room temperature for 16 h. The resulting mixture was then poured into ultrapure MilliQ water (300 mL) and centrifugated at 3000 rpm for 5 min. The solid residue was recovered and washed with fresh milliQ water (500 mL). The supernatant was filtered through a PTFE membrane (0.1 μm). The washing procedure was repeated four times and each time the supernatant was filtered through the PTFE membrane. After the washing steps, the solid material was collected on the PTFE membrane used to filter the supernatant and the reunited fractions were washed with 2-propanol to remove the aqueous traces and dried at 80 °C overnight.

2.3.3. Preparation of base treated materials

500 mg g-CN or CNO were transferred into a glass vial along with an aqueous solution (0.1 M, 10 mL) of the selected base (NaOH, *t*-BuOK, K_2CO_3). The resulting mixture was stirred at room temperature for 16 h. The solid was collected through filtration using a PTFE membrane (0.1 μm). The solid was thoroughly washed with ultrapure milliQ water (3×50 mL) and 2-propanol (10 mL). The so-obtained material was dried at 80 °C overnight.

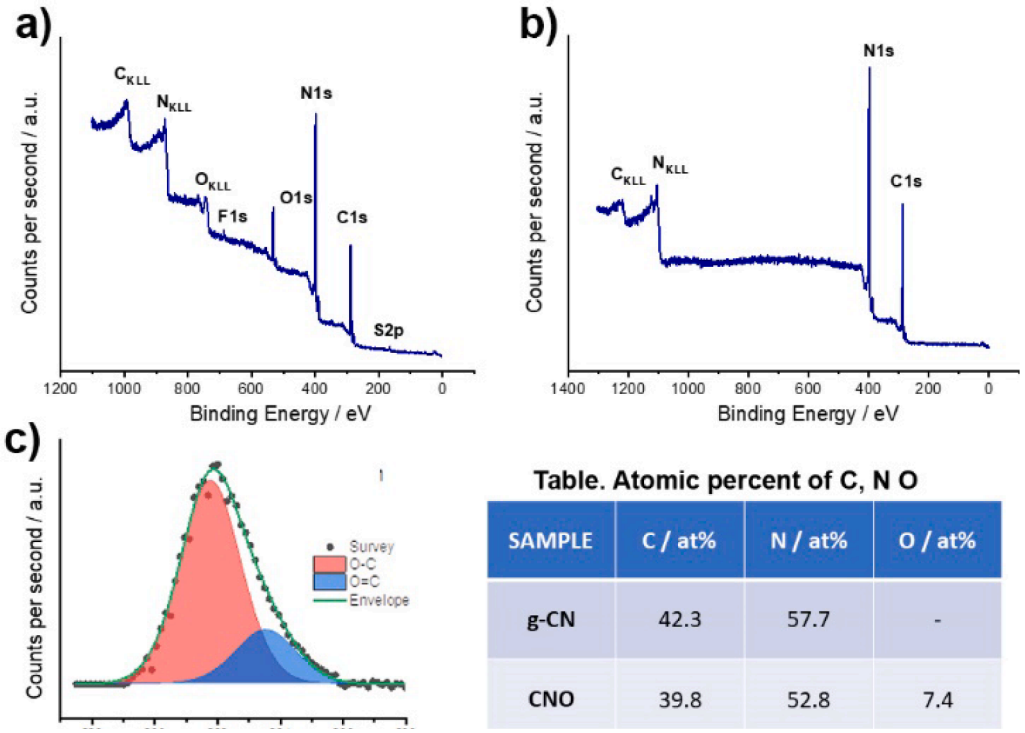

Table. Atomic percent of C, N O

SAMPLE	C / at%	N / at%	O / at%
g-CN	42.3	57.7	-
CNO	39.8	52.8	7.4

Fig. 1. a) XPS survey spectrum of CNO; b) XPS survey spectrum of g-CN; c) high resolution XPS spectrum of CNO in the O1s binding energy range.

2.4. Determination of the intrinsic pH of CNs in water

The appropriate carbon nitride (10 mg) was dispersed in ultrapure MilliQ water (4 mL) and filtered through a PTFE membrane (0.2 µm). The pH of the resulting solution was determined using a pH meter.

2.5. Quantification of the surface basic sites of carbon nitrides

The appropriate carbon nitride (200 mg) was treated with an aqueous solution of HCl (0.1 M, 10 mL) and stirred at room temperature overnight. The resulting mixture was filtered through a PTFE membrane (0.1 µm) and a portion of the so-obtained solution (5 mL) was titrated with NaOH (0.1 M). The resulting amount of titrant at the equivalent point was extrapolated by the linearization of the titration curve and used to determine the degree of functionalization of the material (See SI, Section 3).[22]

2.6. General procedure for the organocatalytic Knoevenagel condensation

The appropriate carbon nitride (5 mg, 5 mg mL^{-1}) was dispersed in acetonitrile (1 mL). Benzaldehydes **1a-f** (0.1 mmol, 1 equiv., 0.1 M) and malononitrile **2a** (0.2 mmol, 2 equiv.) were added to the dispersion. The reaction mixture was stirred either at 25 °C or 70 °C for 2–16 h. The reaction mixture was filtered through sodium sulfate. The solvent was removed under reduced pressure. The production yields listed in Table 1 and Fig. 6 and referred to products **3a-f** were determined by ^{1}H NMR spectroscopy in CDCl3 using 1,1,2-trichloroethylene (0.10 mmol, 9 µL) as the internal standard (I.S.).

3. Results and discussion

The initial g-CN was obtained by thermally treating melamine at 550 °C, as previously reported (Fig. 3a. Then, g-CN was subjected to a strong oxidation protocol using a mixture of nitric and sulfuric acid, affording the oxidized CN material (CNO). A preliminary visual inspection of both materials reveals substantial bleaching of the CNO powder due to the strong oxidative treatment, which likely disrupts the structural organization of the CN motif. This is also indicated by the UV-Vis spectra of g-CN and CNO dispersed in water, where it is observed that the CNO material (black line, left spectrum in Fig. 3c shows a negligible absorption of visible light (λ >400 nm), while the g-CN absorbs up to 500 nm (orange line in Fig. 3c. As known for other carbon nanostructures, such as carbon nanotubes,[23,24] oxidative treatments with sulfonitric mixtures introduce a distribution of oxygenated functionalities including carboxylic acid, hydroxyl, epoxy and ketone groups. X-ray photoelectron spectroscopy (XPS) analysis compares the

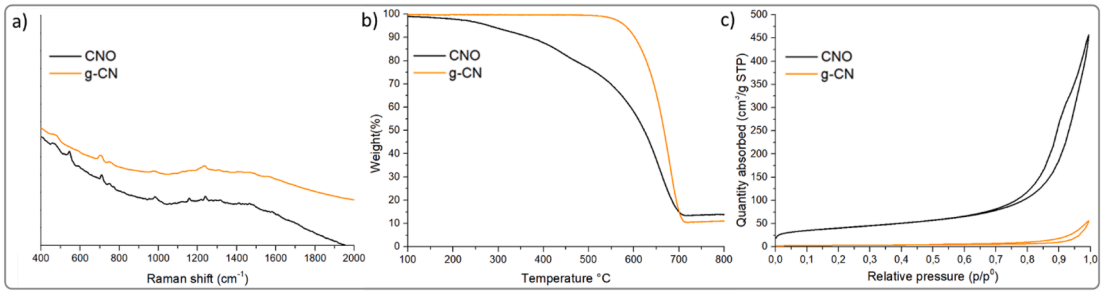

Fig. 2. a) Raman spectra g-CN vs CNO b) TGA of g-CN vs CNO under N_2 atmosphere c) N_2 physisorption isotherms of g-CN and CNO.

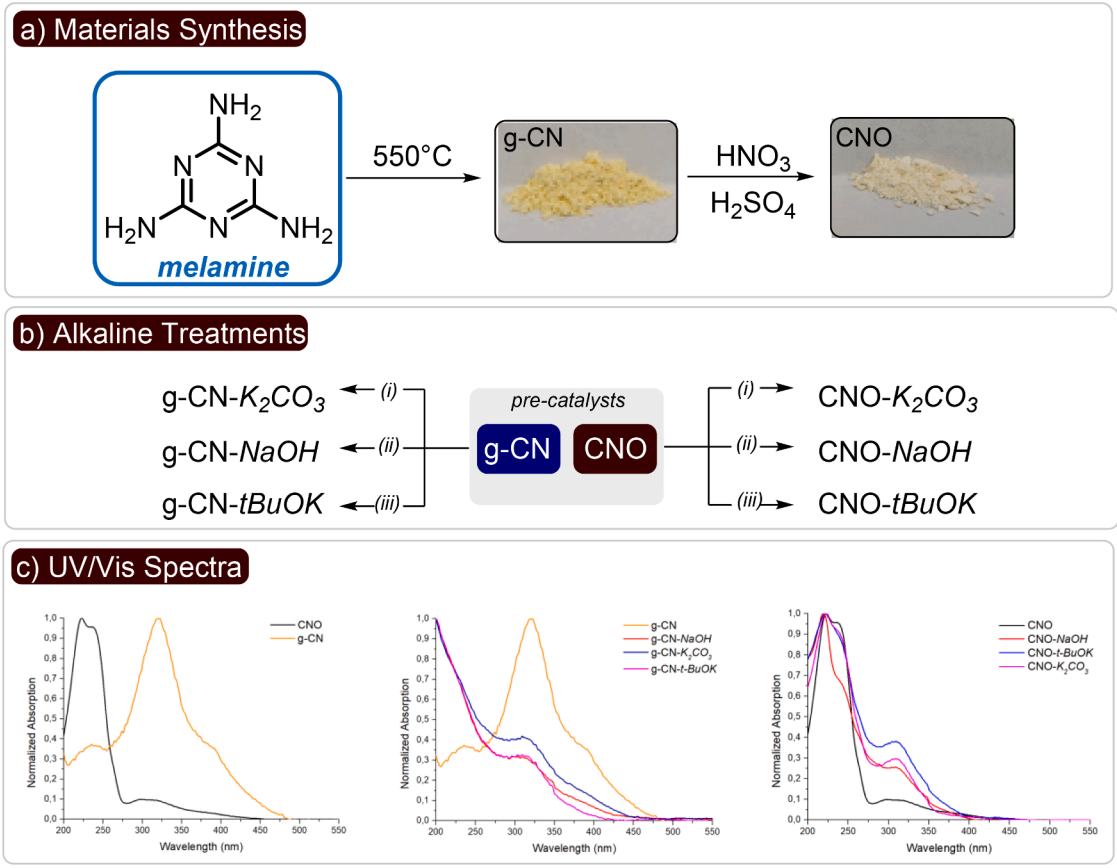

Fig. 3. a) Synthesis and photographs of g-CN and CNO. b) Production of the heterogeneous basic nanocatalysts. Alkaline treatments: (*i*) aqueous solution of potassium carbonate (0.1 M); (*ii*) aqueous solution of sodium hydroxide (0.1 M); (*iii*) aqueous solution of potassium *tert*-butoxide (0.1 M). c) UV/Vis spectra of the studied CNs. The samples were prepared by dispersing 10 mg of the appropriate CN in 5 mL of ultrapure milliQ water and sonicated for 10 min. Then, 50 µL of the resulting suspension was further diluted in 3 mL of milliQ water before recording the optical spectra (quartz cuvettes, 10 mm path length).

spectra of g-CN and CNO, confirming that the oxidation treatment has indeed introduced a significant amount of oxygen (7.4 at%). Deconvolution of the O1s core level shows that that O atoms are present as C—O and C═O species (Fig. 1. Deconvolution data for the peaks relative to N and C confirm the typical patterns of CN materials (Fig. S5).

Thermogravimetric analysis (TGA) is in agreement with the hypothesised functionalized structure, with CNO displaying a multi-step weight loss at an onset temperature of 150 °C, attributed to the combustion of the oxygen-containing groups, this feature is absent in g-CN. In particular, the first weight loss may be assigned to the removal of adsorbed water molecules, more abundant in CNO because of the strong H-bond interaction with the COOH and OH groups.[21] Additionally, Raman analysis provided evidenced of the effect of the oxidation: the heptazine breathing mode, with the characteristic peaks at ~480 and ~700 cm^{-1} are much better defined in CNO as compared to g-CN, this difference being also observed for the peak at 978 cm^{-1}, diagnostic of the C—N in-plane vibration mode.[21,25] Finally, a new peak at ~ 1165 cm^{-1} appears in the CNO materials, which is attributed to the presence of oxygenated functionalities, possibly the OH bending mode.[26] All these features, apart from supporting the introduction of oxygenated groups, suggest that the strong acidic treatment favors an exfoliation of the bulk g-CN by shuffling the planarity of the poly-triazine strands, and the improved de-stacking of the CN sheets is responsible for the improved Raman peak definition. TEM images can be found in SI, Section 9. In agreement with this hypothesis, the investigation of the textural properties by N_2 physisorption shows that the oxidation process results in a significant increase of the surface area when compared with g-CN (Fig. 2c. This well correlates with the hypothesized disruption of long-range planarity of the triazine motifs.

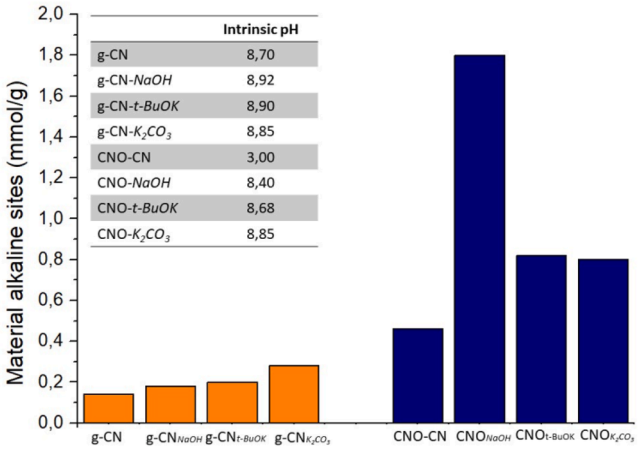

	Intrinsic pH
g-CN	8,70
g-CN-*NaOH*	8,92
g-CN-*t-BuOK*	8,90
g-CN-K_2CO_3	8,85
CNO-CN	3,00
CNO-*NaOH*	8,40
CNO-*t-BuOK*	8,68
CNO-K_2CO_3	8,85

Fig. 4. Total number of surface basic sites and intrinsic pH of the studied CNs.

Specifically, the calculated Brunauer-Emmett-Teller (BET) surface area for g-CN is 17 m^2g^{-1}, in agreement with literature,[27] whereas the surface area for CNO turns out to be 134 m^2g^{-1}. Both g-CN and CNO present type IV isotherms, which indicate presence of mesopores. Fig. 2 shows the comparison of the Raman spectra, TGA and N_2 physisorption analysis for g-CN vs CNO. Supplementary characterization data are available at Figs. S2 and S3.

To endow the materials with base sites for Knoevenagel reaction, g-CN and CNO were treated with aqueous alkaline solutions of both

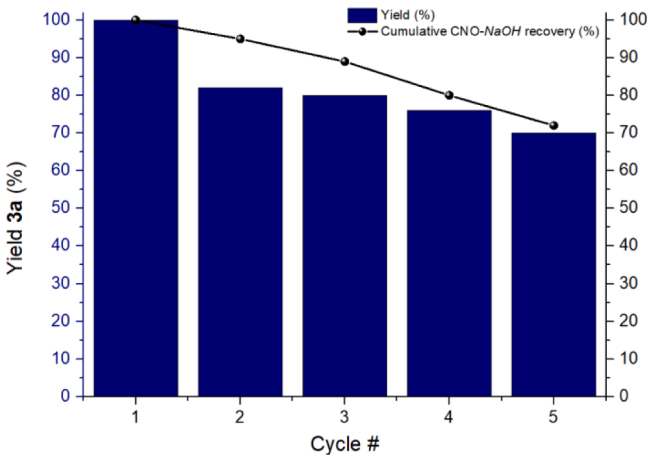

Fig. 5. Catalytic performance of recovered CNO-*NaOH* over five cycles. Yield of product **3a** (blue bars) was determined by ^{1}H NMR using 1,1,2-trichloroethene as the internal standard. CNO-*NaOH* recovery (black line) was determined by weighing the recovered material after centrifugation, washing and drying. (For interpretation of the references to colour in this figure legend, the reader is referred to the web version of this article.)

organic and inorganic bases, namely NaOH, K_2CO_3 and *t*-BuOK (Fig. 3b. It had already been reported by Su et al. that such strong base treatments are needed to activate the surface basic moieties present on the g-CN surface, thus allowing its exploitation as heterogeneous base organocatalyst.[20] As depicted in Fig. 3c, in all cases the deprotonation of g-CN leads to a significant decrease in intensity of the absorption band at 325 nm. Conversely, this absorption band increases on CNO materials upon the alkaline treatment.

Based on TGA and XPS data, the deprotonation of g-CN proceeds with removal of the protons on the lattice N atoms, while for CNO, in addition to the N—H protons, the treatment removes acidic hydrogen from the COOH and OH groups (SI Fig. S2, thus endowing the CNO with a higher density of catalytic sites. In agreement with this hypothesis, the successful deprotonation of the abovementioned functionalities was confirmed by acid/base titration (Fig. 4, SI Section 3).[28] Indeed, CNO-*NaOH* displayed the highest number of surface alkaline sites (1.78 mmol g^{-1}) and the most alkaline intrinsic pH in water (8.9), suggesting that NaOH is the most suitable base for the deprotonation process, presumably removing also the less acidic protons. Conversely, the intrinsic pH of g-CN was already slightly alkaline, so that treatment with bases does not introduce any additional basic sites to a significant extent, and the pH varies only marginally in the three base-treated derivatives.

The feasibility of our hypothesis was tested by reacting benzaldehyde (**1a**) and malononitrile (**2a**) in acetonitrile over 16 h at 70 °C (Table 1. A control experiment confirmed the catalytic nature of the model reaction, since the starting substrates were completely recovered in the absence of any material (entry 1, Table 1. In addition, the use of the pre-catalysts, namely g-CN and CNO, did not lead to the formation of **3a** (entries 2–3, Table 1. Interestingly, we did not observe any reactivity when employing the materials obtained through the alkaline treatments of g-CN (entries 4–6, Table 1. This indicates the absence of reactive basic sites on the surface of these carbon-based nanostructures. On the other hand, the utilization of CNO-K_2CO_3, CNO-*NaOH* and CNO-*tBuOK* (5 mg mL^{-1}) gave **3a** in quantitative yield (entries 7–9, Table 1. This suggests that the strong oxidative treatment (HNO_3/H_2SO_4), that is needed to produce CNO, results in the presence of a high number of surface acidic sites. Then, these sites can be easily deprotonated in the presence of a suitable base, therefore producing efficient heterogeneous basic nanocatalysts. To discern the effect of the specific string base used,

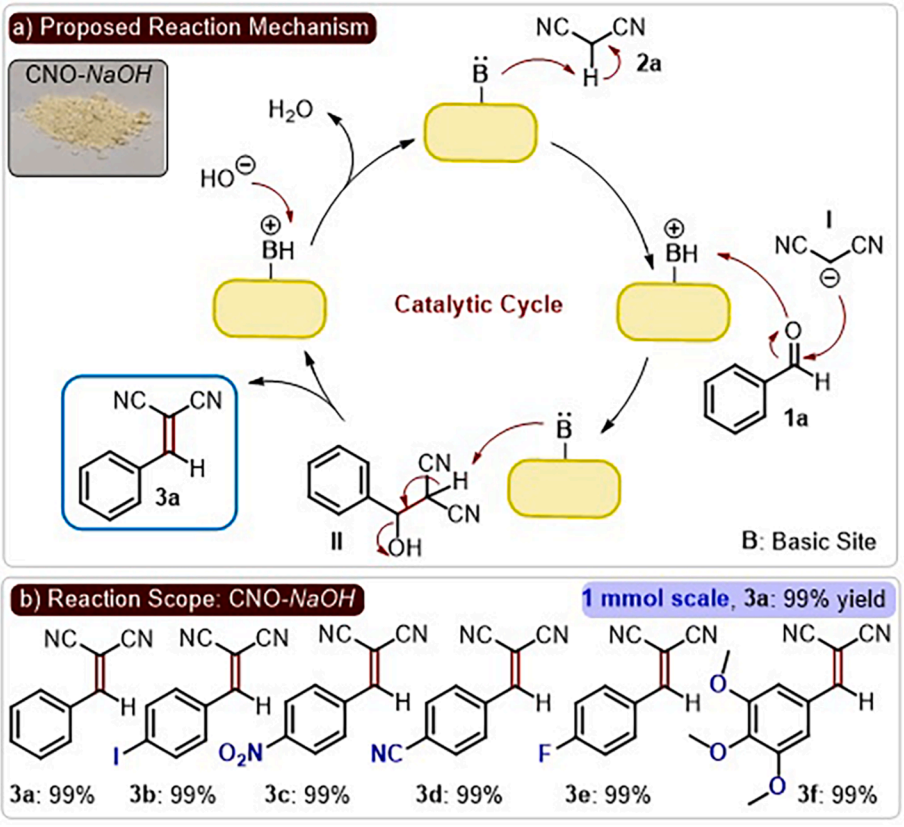

Fig. 6. a) Proposed reaction mechanism which drives the formation of product **3a**. b) Scope: reactions were performed on a 0.1 mmol. Yields determined by ^{1}H NMR spectroscopy using 1,1,2-trichloroethene as the internal standard.

the catalytic tests were run under milder conditions, namely by running the model reaction at 25 °C (entries 10–12, Table 1. As expected on account of the titration experiments, the best performing catalytic system is CNO-*NaOH*, which can form the coupling product with a remarkable 83% yield. Following an optimization study (solvent, time and catalyst loading), section S4 of supporting, the optimized reaction conditions with CNO-*NaOH* as the catalyst were then found (entry 13, Table 1.

We evaluated the recyclability of the CNO-*NaOH* catalyst under the optimized reaction conditions. The abovementioned material was recovered after each run by centrifugation, washed with acetonitrile and used again over five cycles without important loss in reactivity (Fig. 5).

The catalytic cycle that drives the formation of compound **3a** is depicted in Fig. 6a. The mechanism of the Knoevenagel condensation proceeds *via* the generation of the anion **I** by deprotonation of **2a** by the surface basic sites of the catalytic system. The condensation between **I** and **1a** gives the intermediate **II**, which eventually decomposes to afford the final product **3a** and the regenerated catalyst. Moreover, the catalyst proved to be effective in catalyzing the selected organic transformation even at a 1 mmol scale with a quantitative conversion of reagent **1a** into **3a**. The synthetic potential of this catalytic approach was then evaluated by reacting different *para*-substituted benzaldehydes (**1a-f**) with **2a**. Importantly, in all cases we observed the formation of the final products (**3a-f**) in excellent yields, thus showing the high catalytic activity of CNO-*NaOH* (Fig. 6b).

4. Conclusions

In this work, we developed a strategy to make carbon nitride efficient base catalyst, able to drive heterogeneous Knoevenagel couplings between benzaldehydes and malononitrile with quantitiative yield under conventionally adopted conditions and turned out to be highly performant even at lower mg ml^{-1} loading or at lower temperature. The heterogeneous catalytic materials were obtained by a two-step procedure, where g-CN was first strongly oxidized and then treated with strong bases (NaOH, K_2CO_3 and *t*-BuOK). The best catalyst turned out to be CNO-*NaOH*, which is also the one with the highest density of surface basic functionalities, presumably because NaOH is most efficient in deprotonating even less acidic hydrogen. Moreover, the so-designed catalytic system was found to be stable under the reaction conditions and recyclable over five independent cycles. The present study will potentially allow the exploitation of oxidized CN catalyst as pre-catalyst for performing other heterogeneous base catalysis for organic synthesis. For instance, CNO-*NaOH* could also be applied to catalyze transesterification reactions. Alternatively, its precursor, namely CNO, could find application as an heterogenous acid catalyst capable to drive the effective functionalization of carbonyl compounds, olefins, aromatics and so on.[29–31]

Declaration of Competing Interest

The authors declare that they have no known competing financial interests or personal relationships that could have appeared to influence the work reported in this paper.

Acknowledgements

M. M. and G. F. kindly acknowledge the FRA2021, both funded by the University of Trieste. G. F. acknowledges Microgrants 2021 funded by Region FVG (LR 2/2011, ART. 4). M. P. is the AXA Chair for Bionanotechnology (2016–2023). This work was supported by the University of Trieste, INSTM, and the Italian Ministry of Education MIUR (cofin Prot. 2017PBXPN4). Part of this work was performed under the Maria de Maeztu Units of Excellence Program from the Spanish State Research Agency Grant No. MDM-2017-0720. We thank Dr. Paolo Bertoncin for his precious support with TEM analysis.

References

[1] S.E. Denmark, G.L. Beutner, Lewis base catalysis in organic synthesis (2008), https://doi.org/10.1002/anie.200604943.
[2] A. Kondoh, A. Iino, S. Ishikawa, T. Aoki, M. Terada, Efficient Synthesis of Polysubstituted Pyrroles Based on [3+2] Cycloaddition Strategy Utilizing [1,2]-Phospha-Brook Rearrangement under Brønsted Base Catalysis, Chem. Eur. J. 24 (57) (2018) 15246–15253, https://doi.org/10.1002/chem.v24.5710.1002/chem.201803809.
[3] A. Kondoh, C. Ma, M. Terada, Synthesis of diarylalkanes through an intramolecular/intermolecular addition sequence by auto-tandem catalysis with strong Brønsted base, Chem. Commun. 56 (74) (2020) 10894–10897, https://doi.org/10.1039/D0CC04512H.
[4] M.J. Zacuto, Synthesis of Acrylamides via the Doebner-Knoevenagel Condensation, J. Org. Chem. 84 (10) (2019) 6465–6474, https://doi.org/10.1021/acs.joc.9b0045010.1021/acs.joc.9b00450.s001.
[5] N. Mase, T. Horibe, Organocatalytic knoevenagel condensations by means of carbamic acid ammonium salts, Org. Lett. 15 (8) (2013) 1854–1857, https://doi.org/10.1021/ol400462d.
[6] J.N. Appaturi, R. Ratti, B.L. Phoon, S.M. Batagarawa, I.U. Din, M. Selvaraj, R. J. Ramalingam, A review of the recent progress on heterogeneous catalysts for Knoevenagel condensation, Dalt. Trans. 50 (13) (2021) 4445–4469, https://doi.org/10.1039/D1DT00456E.
[7] K. Ikeue, N. Miyoshi, T. Tanaka, M. Machida, Ca-containing mesoporous silica as a solid base catalyst for the knoevenagel condensation reaction, Catal. Letters. 141 (6) (2011) 877–881, https://doi.org/10.1007/s10562-011-0613-3.
[8] H. Jia, Y. Zhao, P. Niu, N. Lu, B. Fan, R. Li, Amine-functionalized MgAl LDH nanosheets as efficient solid base catalysts for Knoevenagel condensation, Mol. Catal. 449 (2018) 31–37, https://doi.org/10.1016/j.mcat.2018.02.004.
[9] G. Tuci, L. Luconi, A. Rossin, E. Berretti, H. Ba, M. Innocenti, D. Yakhvarov, S. Caporali, C. Pham-Huu, G. Giambastiani, Aziridine-Functionalized Multiwalled Carbon Nanotubes: Robust and Versatile Catalysts for the Oxygen Reduction Reaction and Knoevenagel Condensation, ACS Appl. Mater. Interfaces. 8 (2016) 30099–30106, https://doi.org/10.1021/acsami.6b09033.
[10] B. Gholipour, S. Shojaei, S. Rostamnia, M.R. Naimi-Jamal, D. Kim, T. Kavetskyy, N. Nouruzi, H.W. Jang, R.S. Varma, M. Shokouhimehr, Metal-free nanostructured catalysts: sustainable driving forces for organic transformations, Green Chem. 23 (2021) 6223–6272, https://doi.org/10.1039/d1gc01366a.
[11] X. Li, B. Lin, H. Li, Q. Yu, Y. Ge, X. Jin, X. Liu, Y. Zhou, J. Xiao, Carbon doped hexagonal BN as a highly efficient metal-free base catalyst for Knoevenagel condensation reaction, Appl. Catal. B Environ. 239 (2018) 254–259, https://doi.org/10.1016/j.apcatb.2018.08.021.
[12] B. Sakthivel, A. Dhakshinamoorthy, Chitosan as a reusable solid base catalyst for Knoevenagel condensation reaction, J. Colloid Interface Sci. 485 (2017) 75–80, https://doi.org/10.1016/j.jcis.2016.09.020.
[13] K.S. Egorova, V.P. Ananikov, Which Metals are Green for Catalysis? Comparison of the Toxicities of Ni, Cu, Fe, Pd, Pt, Rh, and Au Salts, Angew. Chem. Int. Ed. 55 (40) (2016) 12150–12162, https://doi.org/10.1002/anie.201603777.
[14] F. Longobardo, G. Gentile, A. Criado, A. Actis, S. Colussi, V. Dal Santo, M. Chiesa, G. Filippini, P. Fornasiero, M. Prato, M. Melchionna, Tailored amorphization of graphitic carbon nitride triggers superior photocatalytic C-C coupling towards the synthesis of perfluoroalkyl derivatives, Mater. Chem. Front. 5 (19) (2021) 7267–7275, https://doi.org/10.1039/D1QM01077H.
[15] G. Filippini, F. Longobardo, L. Forster, A. Criado, G. Di Carmine, L. Nasi, C. D. Agostino, M. Melchionna, P. Fornasiero, M. Prato, Light-driven, heterogeneous organocatalysts for C – C bond formation toward valuable perfluoroalkylated intermediates, Sci. Adv. 6 (2020) eabc9923, https://doi.org/10.1126/sciadv.abc9923.
[16] M. Antonietti, N. Lopez-Salas, A. Primo, Adjusting the Structure and Electronic Properties of Carbons for Metal-Free Carbocatalysis of Organic Transformations, Adv. Mater. 31 (13) (2019) 1805719, https://doi.org/10.1002/adma.v31.1310.1002/adma.201805719.
[17] C. Rosso, G. Filippini, A. Criado, M. Melchionna, P. Fornasiero, M. Prato, Metal-Free Photocatalysis: Two-Dimensional Nanomaterial Connection toward Advanced Organic Synthesis, ACS Nano. 15 (2021) 3621–3630, https://doi.org/10.1021/acsnano.1c00627.
[18] N.D. Shcherban, P. Mäki-Arvela, A. Aho, S.A. Sergiienko, P.S. Yaremov, K. Eränen, D.Y. Murzin, Melamine-derived graphitic carbon nitride as a new effective metal-free catalyst for Knoevenagel condensation of benzaldehyde with ethylcyanoacetate, Catal, Sci. Technol. 8 (11) (2018) 2928–2937, https://doi.org/10.1039/C8CY00253C.
[19] M.B. Ansari, H. Jin, M.N. Parvin, S.-E. Park, Mesoporous carbon nitride as a metal-free base catalyst in the microwave assisted Knoevenagel condensation of ethylcyanoacetate with aromatic aldehydes, Catal. Today. 185 (1) (2012) 211–216, https://doi.org/10.1016/j.cattod.2011.07.024.
[20] F. Su, M. Antonietti, X. Wang, Mpg-C 3N 4 as a solid base catalyst for Knoevenagel condensations and transesterification reactions, Catal, Sci. Technol. 2 (2012) 1005–1009, https://doi.org/10.1039/c2cy00012a.

[21] P. Choudhary, A. Bahuguna, A. Kumar, S.S. Dhankhar, C.M. Nagaraja, V. Krishnan, Oxidized graphitic carbon nitride as a sustainable metal-free catalyst for hydrogen transfer reactions under mild conditions, Green Chem. 22 (15) (2020) 5084–5095, https://doi.org/10.1039/D0GC01123A.
[22] G. Gran, Determination of the equivalence point in potentiometric titrations, Part II, Analyst. 77 (1952) 661–671, https://doi.org/10.1039/AN9527700661.
[23] G. Valenti, A. Boni, M. Melchionna, M. Cargnello, L. Nasi, G. Bertoni, R.J. Gorte, M. Marcaccio, S. Rapino, M. Bonchio, P. Fornasiero, M. Prato, F. Paolucci, Co-axial heterostructures integrating palladium/titanium dioxide with carbon nanotubes for efficient electrocatalytic hydrogen evolution, Nat. Commun. 7 (2016) 1–8, https://doi.org/10.1038/ncomms13549.
[24] S. Gómez, N.M. Rendtorff, E.F. Aglietti, Y. Sakka, G. Suárez, Surface modification of multiwall carbon nanotubes by sulfonitric treatment, Appl. Surf. Sci. 379 (2016) 264–269, https://doi.org/10.1016/j.apsusc.2016.04.065.
[25] J. Xu, L. Zhang, R. Shi, Y. Zhu, Chemical exfoliation of graphitic carbon nitride for efficient heterogeneous photocatalysis, J. Mater. Chem. A. 1 (2013) 14766–14772, https://doi.org/10.1039/c3ta13188b.
[26] N. Lebrun, P. Dhamelincourt, C. Focsa, B. Chazallon, J.L. Destombes, D. Prevost, Raman analysis of formaldehyde aqueous solutions as a function of concentration, J. Raman Spectrosc. 34 (6) (2003) 459–464, https://doi.org/10.1002/(ISSN)1097-455510.1002/jrs.v34:610.1002/jrs.1025.
[27] Z. Li, Y. Wu, G. Lu, Highly efficient hydrogen evolution over Co(OH)2 nanoparticles modified g-C3N4 co-sensitized by Eosin Y and Rose Bengal under Visible Light Irradiation, Appl. Catal. B Environ. 188 (2016) 56–64, https://doi.org/10.1016/j.apcatb.2016.01.057.
[28] H. Ren, E. Cunha, Q. Sun, Z. Li, I.A. Kinloch, R.J. Young, Z. Fan, Surface functionality analysis by Boehm titration of graphene nanoplatelets functionalized: Via a solvent-free cycloaddition reaction, Nanoscale Adv. 1 (2019) 1432–1441, https://doi.org/10.1039/c8na00280k.
[29] T. Akiyama, Stronger Brønsted Acids 107 (2007) 5744–5758.
[30] M. Garrido, L. Gualandi, S. Di Noja, G. Filippini, S. Bosi, M. Prato, Synthesis and applications of amino-functionalized carbon nanomaterials, Chem. Commun. 56 (84) (2020) 12698–12716, https://doi.org/10.1039/D0CC05316C.
[31] C. Rosso, G. Filippini, M. Prato, Carbon dots as nano-organocatalysts for synthetic applications, ACS Catal. 10 (15) (2020) 8090–8105, https://doi.org/10.1021/acscatal.0c01989.